Electronic Supplementary Information

An AIE luminogens-Based Electropolymerized Film: Ultrasensitive Fluorescent Probe for TNP and Fe^{3+} in Water

Hongmin Hao,[‡a] Chao Xu,[‡a] Haiyuan Luo,[a] Jinglian Yang,[a] Cong Liu,*[a] Bingjia Xu,[a] Guang Shi,[a] Xiaobo Xing[b] and Zhenguo Chi[c,d]

a.Key Laboratory of Theoretical Chemistry of Environment, Ministry of Education, School of Chemistry, South China Normal University, Guangzhou 510006, China

b. Centre for Optical and Electromagnetic Research, South China Academy of Advanced Optoelectronics, South China Normal University, Guangzhou 510006, China

c. Key Laboratory for Polymeric Composite and Functional Materials of Ministry of Education, Sun Yat-sen University, Guangzhou 510275, China.

d. State Key Laboratory of Optoelectronic Materials and Technologies, Sun Yat-sen University, Guangzhou 510275, China

Contents:

1. Experimental Procedures

General

All chemicals and solvents were used as received from commercial sources, unless otherwise noted. tetrahydrofuran (THF) dried and distilled under argon atmosphere. ^{1}H and ^{13}C-NMR spectra were obtained using a Varian AS600 MHz NMR spectrometer (Varian, Inc., Palo Alto, CA, USA) with $CDCl_3$ solvent and tetramethylsilane (TMS) as internal standard. Mass spectra (MS) were recorded on a Thermo MAT95XP-HRMS spectrometer (Thermo Fisher Scientific Inc., Waltham, MA, USA). Elemental analysis (EA) was obtained on a Vario elemental analysis cube (Elementar Analysensysteme GmbH, Hanau, Germany). Fluorescence spectra were obtained on an FLS980 spectrometer (Edinburgh Instruments Ltd., UK). Ultraviolet-visible (UV-Vis) absorption spectrum was obtained on a Hitachi U-3900 spectrophotometer (Hitachi Instruments, Inc., Tokyo, Japan). Fourier transform-infrared (FT-IR) spectra were measured using a Bruker Vector 33 spectrometer (KBr pellet; Bruker Corp., Billerica, MA, USA). Dynamic light scattering measurement was using a Particle Size Analyzer-Zetasizer Nano ZS90. The film thickness was measured on a Veeco Dektak 150 profilometer. X-ray photoelectron spectroscopy (XPS) was carried out on an Axis Ultra DLD instrument (Kratos Analytical, Ltd., Manchester, UK) with photoelectrons generated by the nonmonochromatic Al-K_α irradiation (1486.6 eV). Powder X-ray diffraction (XRD) patterns were recorded by a Ultima IV X-ray diffractometer (Rigaku Corp., Tokyo, Japan) in a scanning rate of 4° (2θ)/min at 293K. Atomic force microscopic (AFM) experiments were performed on a SPA 400 (Seiko Instruments USA, Inc., CA, USA) with SPI 3800 probe station. Scanning electron microscopy (SEM) images were measured by a Gemini 500 field emission scanning electron microscope (Carl Zeiss AG, Oberkochen, Germany). Transmission electron microscopic images (TEM) were recorded on a JEM-3010 electron microscope (JEOL Ltd., Tokyo, Japan) with an acceleration voltage of 300 kV. EP films were prepared using a cyclic voltammetry (CV) method with a CHI760D electrochemical workstation (CH Instruments, Inc., Austin, TX, USA). Indium-tin oxide (ITO)-coated glass, Ag/Ag^+ and nonaqueous electrode, and titanium plate were used as the working, reference, and counter electrodes, respectively. EP films were produced on ITO-coated glass by multicyclic CV of PhTPECz (0.6 mg/mL) in a mixture of acetonitrile/dichloromethane (DCM; 1/4, v/v) containing the supporting electrolyte of tetrabutylammonium hexafluorophosphate (0.1 M) at room temperature.

Theoretical Calculations

Conformations were optimized employing density functional theory (DFT) at the B3LYP/6-31G (d, p) level. Calculations were carried out using the Gaussian 16 package and the frontier molecular orbital demonstrated using Gauss View 6 software.

Synthetic procedures

PhTPECz: Compound 1 (1.16 g, 1.62 mmol), compound 2 (0.22 g, 0.35 mmol), and a catalyst, $Pd(dpdf)Cl_2$, (0.01 g，0.01 mmol) were added to 25 mL of THF under an argon atmosphere and stirred. After 7 mL of $NaHCO_3$ solution (2 M) was added dropwise to the solution in a three-necked round bottom flask, the mixture was stirred at 70°C for 48 h, and then cooled to room temperature. After removing THF under reduced pressure, the mixture was then extracted with DCM and deionized water. The organic phase was collected, filtered, and dried with $MgSO_4$ overnight and DCM removed under reduced pressure. The obtained solid was purified by silica gel column chromatography using DCM/petroleum ether (PE; 1/1, v/v) as an eluent to obtain a yellow solid (0.52 g, 55%).

^{1}H-NMR (600 MHz, $CDCl_3$) δ 8.19 (dd, J = 15.3 and 7.7 Hz, 16H), 7.75–7.69 (m, 8H), 7.63 (dd, J = 15.0 and 8.3 Hz, 16H), 7.60 –7.55 (m, 16H), 7.53 (s,8H), 7.52–7.41 (m, 32H), 7.34 (dt, J = 15.1 and 7.2 Hz, 16H), 7.27 (d, J = 13.3 Hz,4H), 7.25–7.20 (m, 16H);^{13}C-NMR (151 MHz, $CDCl_3$) δ 141.99, 140.93, 139.96, 139.73, 138.17, 137.31, 136.18, 135.10, 131.03, 129.16, 128.04, 126.37, 125.84, 125.49, 125.08, 122.51, 119.43, 119.11, and 108.86; MS (MALDI-TOF), m/z: 2671.464 ($[M+H]^+$ calc'd for $C_{202}H_{132}N_8$, 2669.057); Anal. Calc. for $C_{202}H_{132}N_8$: C 90.82, H 4.98, and N 4.19 and found: C 90.84, H 5.12, and N 4.03%.

Detection method

To explore the sensing properties of PhTPECz monomer and polyPhTPECz EP films, the fluorescence spectra of PhTPECz and polyPhTPECz EP films were recorded by adding different concentrations of quenchers to solutions. The polyPhTPECz EP films were immersed in an aqueous solution, after adding NACs or iron chloride for 5 s, then, the fluorescence measurement was taken. The following NACs were chosen for the fluorescence sensing studies: 2,4,6-trinitrophenol (TNP), 2,4-dinitroplenol (DNP), 2-nitrophenol (NP), 2,4,6-trinitrotoluene (TNT), 2-nitrotoluene (2-NT), and nitrobenzene (NB). The probe sensitivity was estimated by the Stern-Volmer constant (K_{sv}), which was calculated from the slope of the Stern-Volmer curve, $I_0/I\text{-}1=K_{sv}[Q]$. The I_0 was the original fluorescence intensity, I the fluorescence intensity after exposure in quencher, and $[Q]$ the quencher concentration. Calculation of the limit of detection (LOD) was based on the fluorescence titration using the equation LOD = $3\sigma/m$, where σ was the standard deviation of the blank solution and m the calibration curve slope between the fluorescence intensity change and quencher concentration.

Probe utility in TNP vapor detection was explored by placing TNP powder into the bottom of quartz cell for 60 min. After a constant TNP vapor was reached, the polyPhTPECz EP film was exposed to the saturated TNP vapor at room temperature and the fluorescence spectrum recorded at different time intervals.

Reusability was demonstrated, after exposing a film to TNP solution and vapor, by washing the polyPhTPECz film with ethanol for three times, dried under vacuum for 50°C for 4 h, and then reused in the next-round sensing to explore reusability. Film reusability in Fe^{3+} detection was explored by washing EP films with ethylene diaminetetraacetic acid after being exposed to Fe^{3+} and then dried and used again to detect Fe^{3+}.

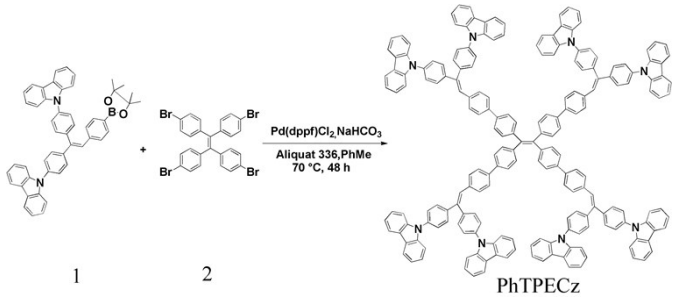

Scheme S1. Synthetic routes for PhTPECz.

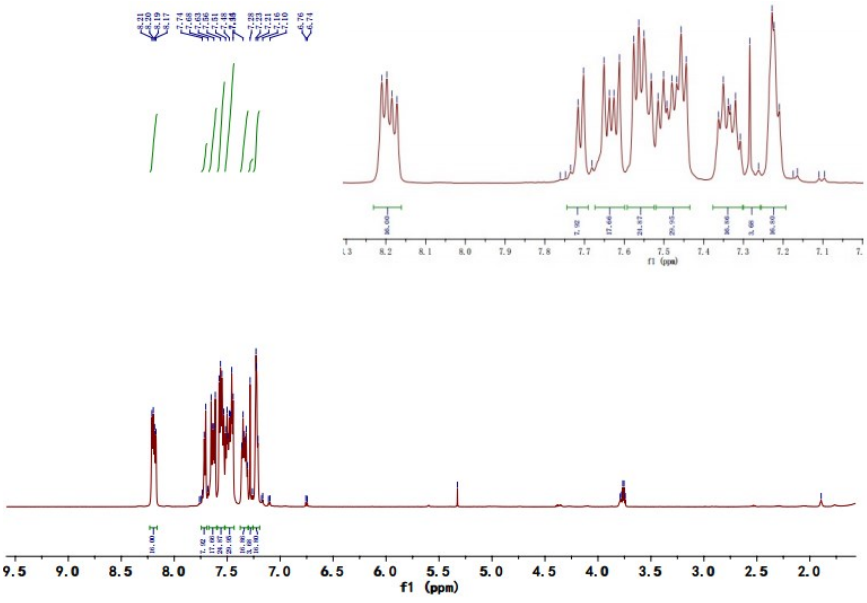

Figure S1. The ^{1}H NMR spectrum of PhTPECz

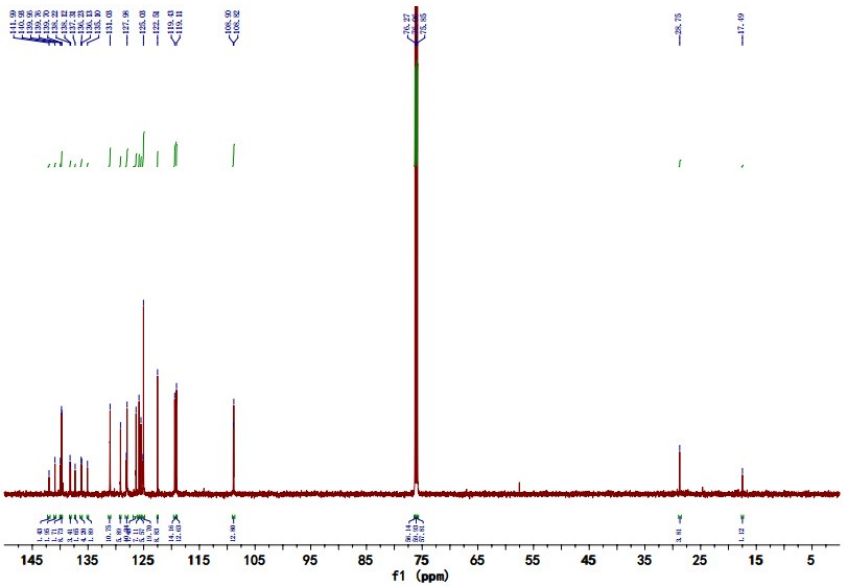

Figure S2 The ^{13}C NMR spectrum of PhTPECz

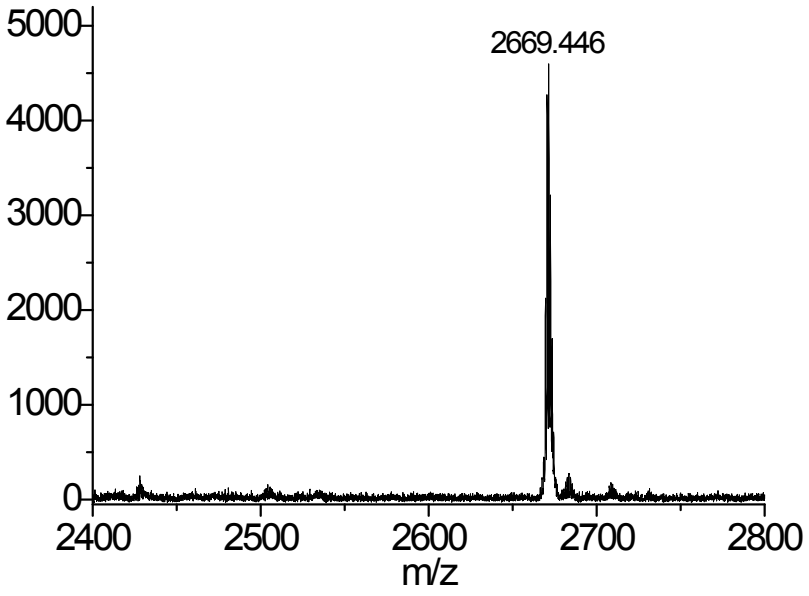

Figure S3 The MS (MALDI-TOF) spectrum of PhTPECz

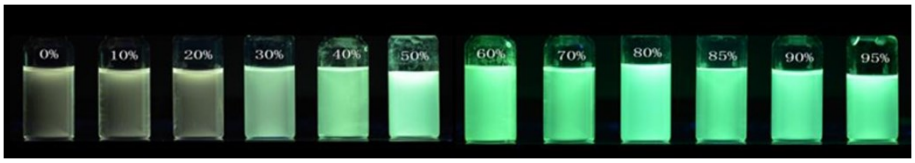

Figure S4. The emission images of PhTPECz in THF and THF/water mixtures with different water fractions

(under the illumination of 365 nm UV light at room temperature).

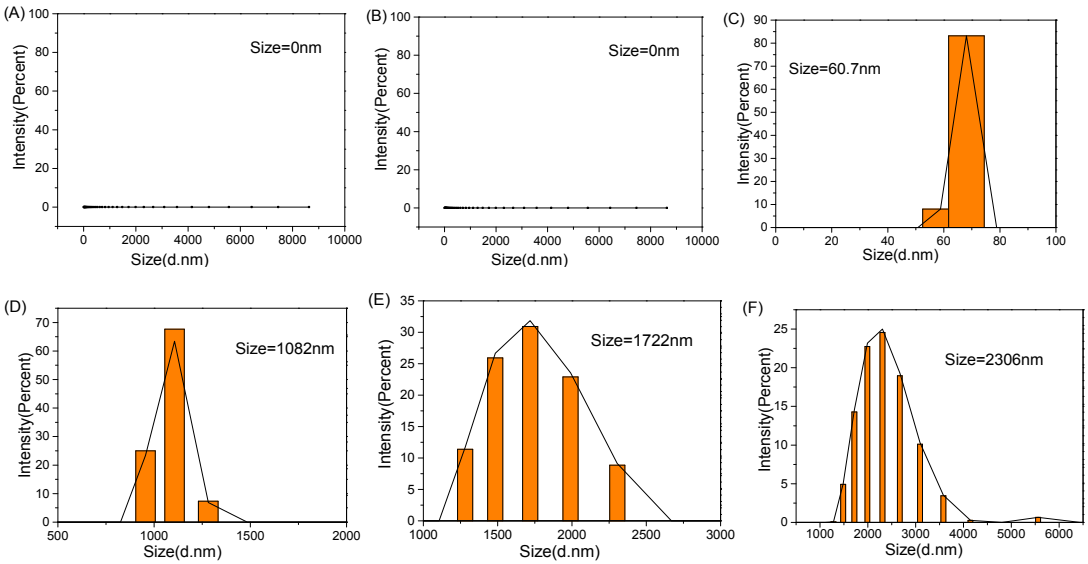

Figure S5. Particle size of PhTPECz aggregates formed in water/THF (v/v) mixture: (A)0:100 (B)10:90 (C)20:80 (D)30:70 (E)40:60 (F)80:20.

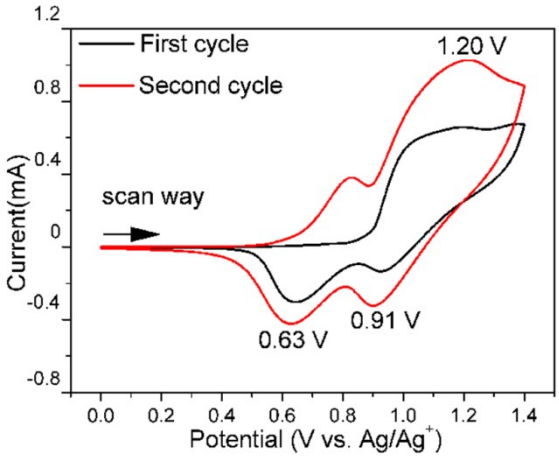

Figure S6. CV profile of the first two cycles of a solution of PhTPECz in acetonitrile/CH_2Cl_2 (1/4 V/V) in the presence of $TBAPF_6$ as electrolyte at 25°C. (0~1.4 V, 60mV/s).

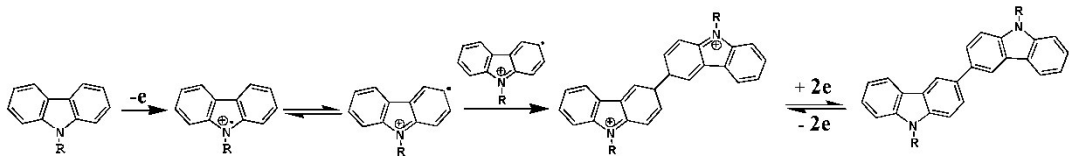

Figure S7. Schematic diagram of carbazole coupling reaction.

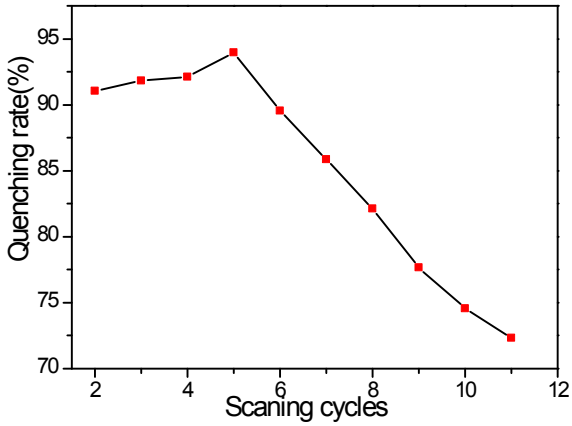

Figure S8.The fluorescence response of polyPhTPECz EP films exposed to TNP solutions (50 μM) vs the scaning cycles of CV method.

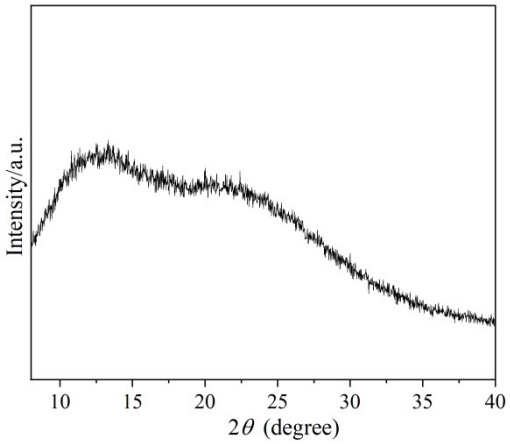

Figure S9. XRD pattern of the polyPhTPECz films.

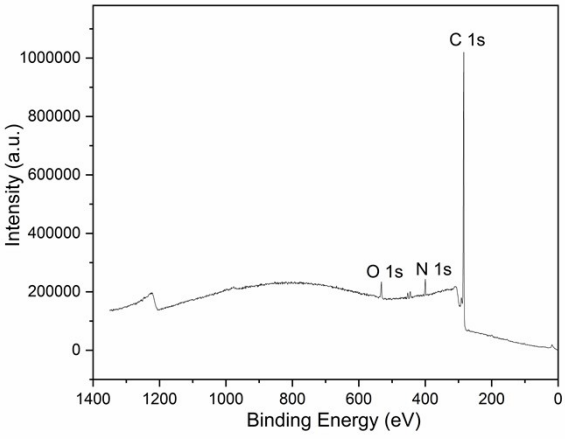

Figure S10. Low-resolution XPS survey spectra of polyPhTPECz films.

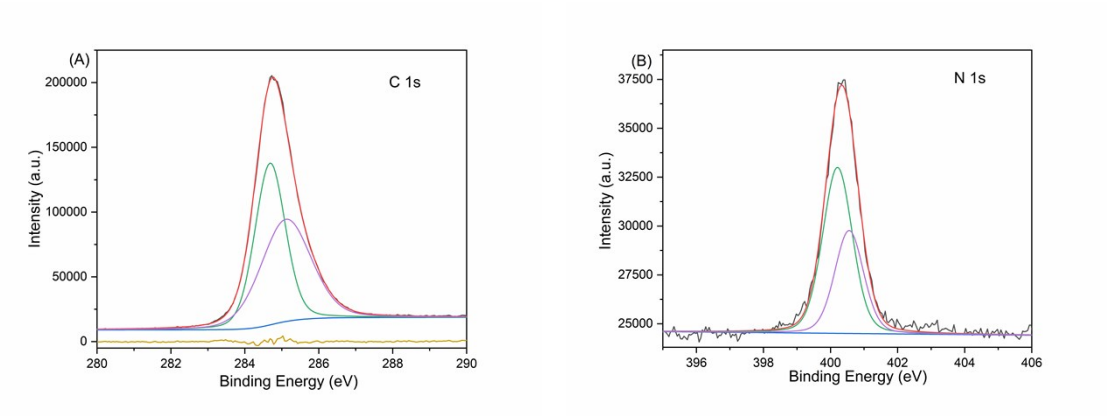

Figure S11. High-resolution XPS spectra of polyPhTPECz films: (A) C 1s, (B) N 1s.

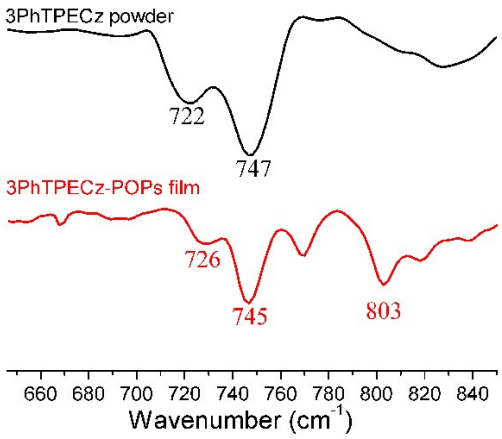

Figure S12. FT-IR spectra of the polyPhTPECz film (red curve) and PhTPECz monomer (black curve).

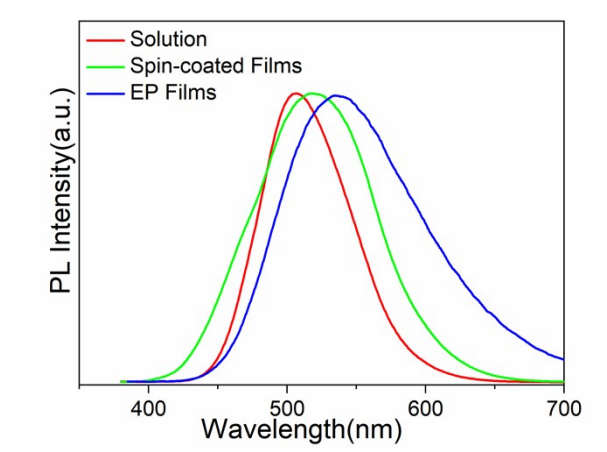

Figure S13. The fluorescence spectra of PhTPECz solution, spin-coated film, and polyPhTPECz EP films.

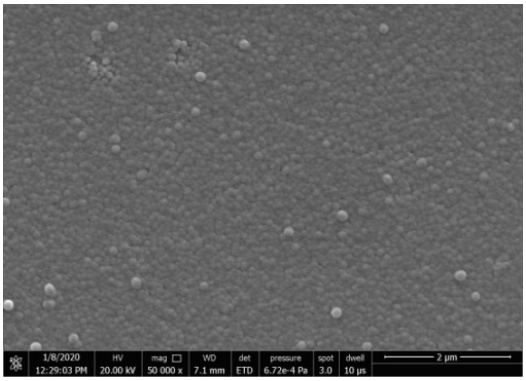

Figure S14. SEM image of the polyPhTPECz EP films.

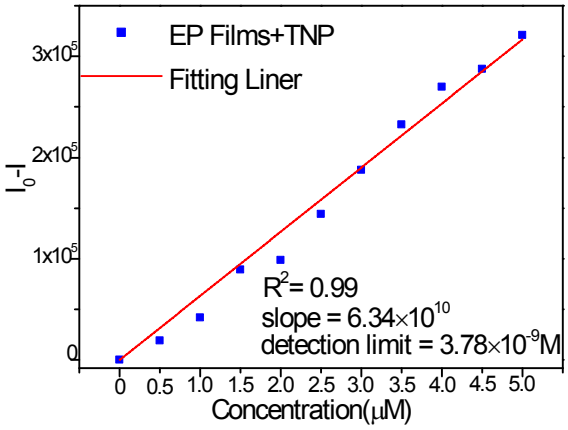

Figure S15.The titration curves of EP films in TNP aqueous solutions.

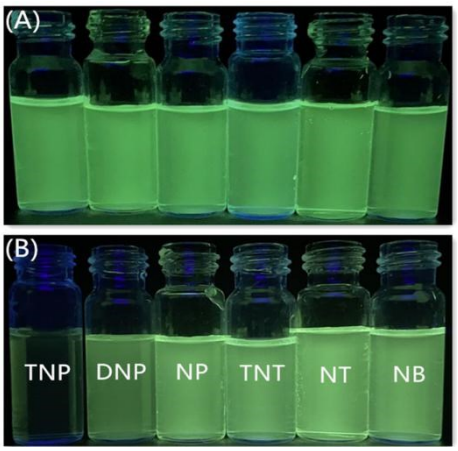

Figure S16. Photographs of PhTPECz monomer molecular solution added with different explosives (100uM) under 365nm ultraviolet light

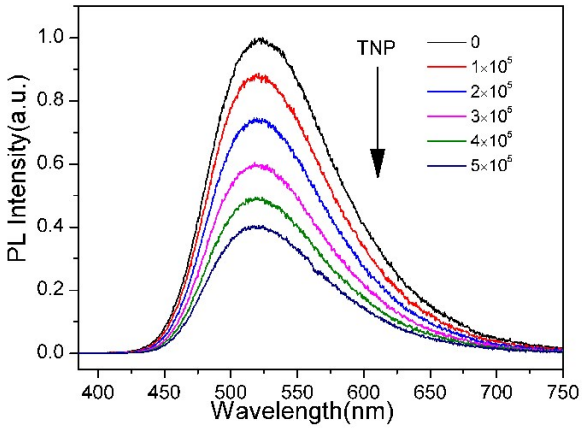

Figure S17. The fluorescence spectra of PhTPECz (1 μM in H_2O/THF, v/v=8/2) recorded upon the addition of TNP dissolved in water from 0 to 50 μM.

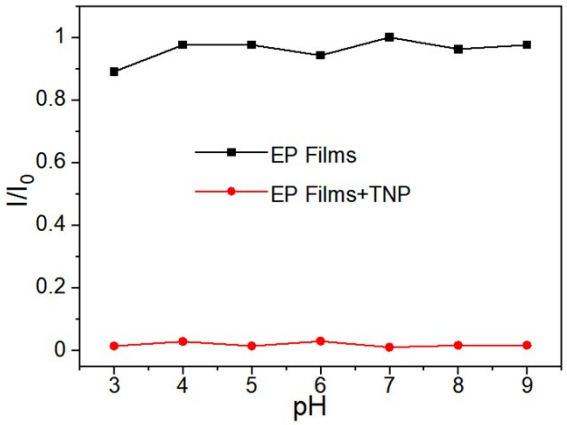

Figure S18. Relative fluorescence intensity of polyPhTPECz EP films and after the addition of TNP in aqueous solution as a function of different pH values (3-9).

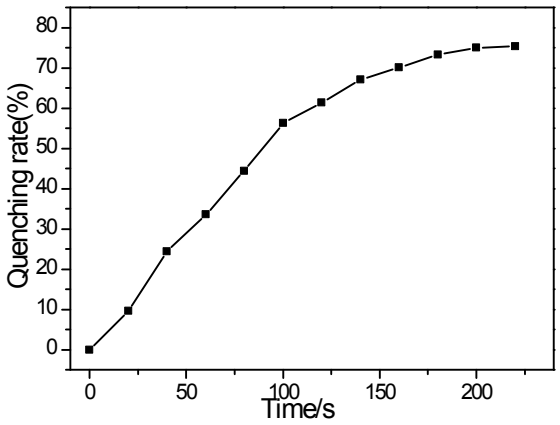

Figure S19. time-dependent fluorescence quenching studies of EP films in saturated TNP vapor phase.

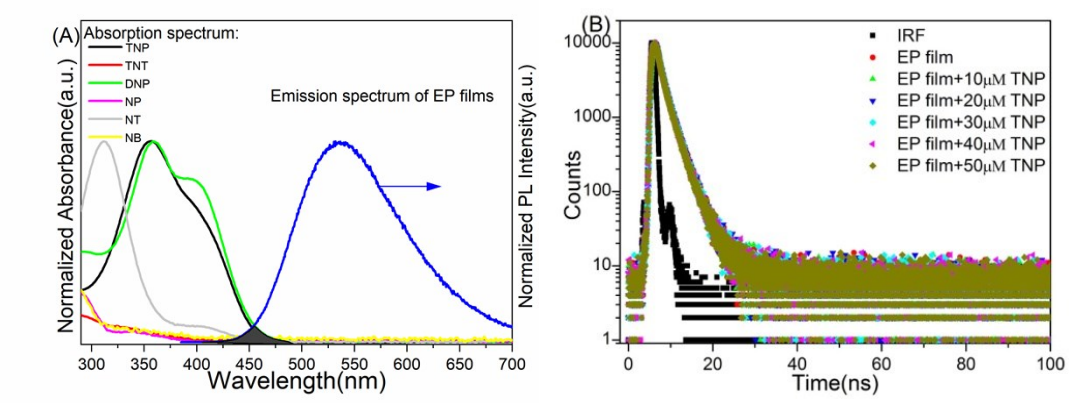

Figure S20. (A)The UV-vis absorption spectra of nitroarenes and fluorescence emission spectrum of polyPhTPECz EP films. (B)Time-resolved fluorescence spectra of polyPhTPECz EP films before and after addition of different concentration of TNP.

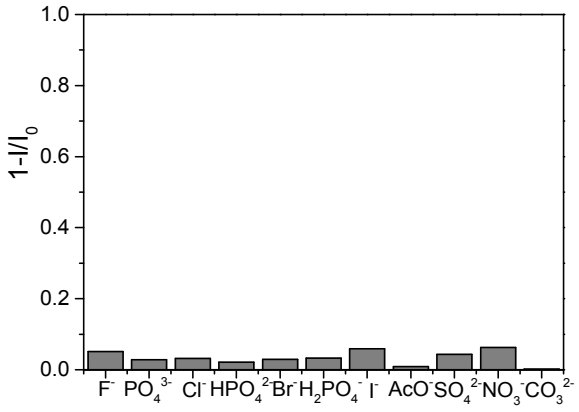

Figure S21. Quenching rate of polyPhTPECz EP films with different anion aqueous solutions (1×10^{-4} M)

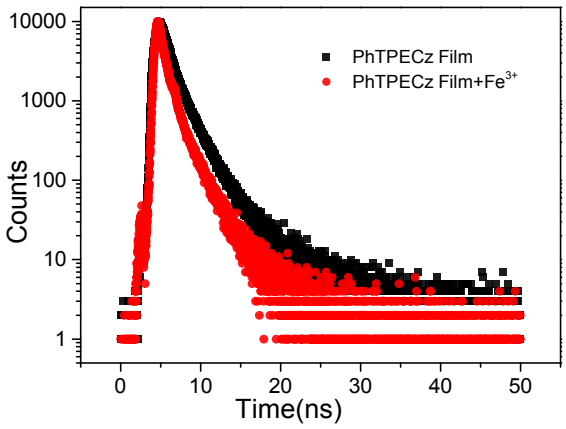

Figure S22. The fluorescence lifetime decay curves of the polyPhTPECz films with or without the addition of Fe^{3+}.

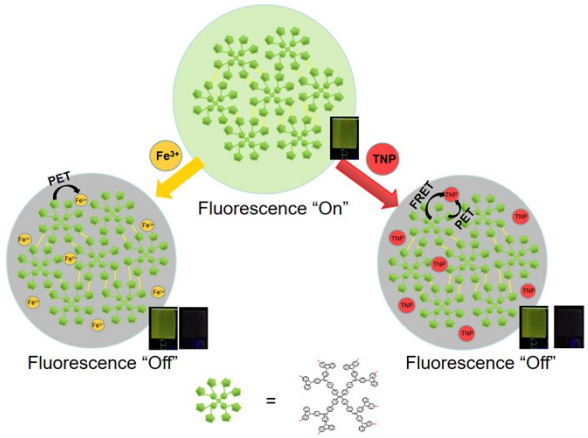

Figure S23. The scheme of sensing mechanism of polyPhTPECz to TNP and Fe^{3+}

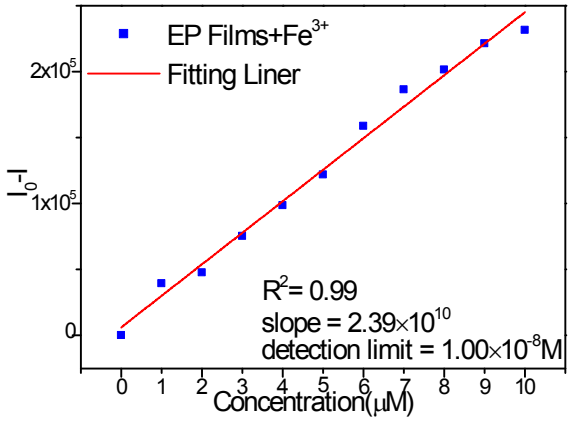

Figure S24. The titration curves of polyPhTPECz EP films in the Fe^{3+} aqueous solution.

Table S1 XPS data showing the binding energy for different elements present in the polyPhTPECz EP films.

Sample	C 1s		N1s	
	C-C	C-N	C-N	N^+
Ep films	284.7	285.1	400.2	400.6

Table S2 Fluorescence quenching data for TNP vapor from different literature.

Sensing material	Fluorescence quenching rate (exposure time)		Reference
TCzDPAn film	30% (60 s)	70% (240 s)	1
TCBzC	38.6% (120 s)	45.5% (300 s)	2
S1	21% (120 s)	80% (600 s)	3
F5 thin film	40% (60 s)	91% (210 s)	4
P4 thin film	37% (60 s)	81% (540 s)	5
polyPhTPECz film	32% (60 s)	73% (180 s)	This work

Table S3 Fluorescence quenching data for detecting Fe^{3+}.

Sensing material	Type of sensor	Detecting system	K_{sv}	LOD	Reference
PYTPAG2 films	film	aqueous solution	$4.5\times10^4\ M^{-1}$	0.085 μM	6
Sensor 1	solution	aqueous solution	$4.31\times10^3\ M^{-1}$	6.95 μM	7
T3	solution	aqueous solution	$1.8\times10^6\ M^{-1}$	0.36 μM	8
Probe 1	solution	aqueous solution	×	0.186 μM	9
DPYBT	solution	THF solution	×	3.04 μM	10
FeP-1	solution	aqueous media	×	0.8 ppb (14 nM)	11
Fe_3O_4@ZnO@L-Cys	nanoparticles	water	×	5 nM	12
Phen-MDI-CA	Solution	water	×	2.6 ppb (46 nM)	13
CD-based fluorescent probe	solution	buffer solution	×	0.28 μM	14
polyPhTPECz film	film		$7.82\times10^4\ M^{-1}$	10.0 nM	This work

REFERENCES

1 H. Hao, H. Luo, A. Yi, C. Liu, B. Xu, G. Shi and Z. Chi, A multifunctional luminescent network film electrochemically deposited from a new AIEE emitter for OLEDs and explosive detection, *Organic Electronics*, 2019, 69, 281-288.

2 H. Ma, F. Li, L. Yao, Y. Feng, Z. Zhang and M. Zhang, Dual-emissive electropolymerization films for the ratiometric fluorescence detection of TNT and TNP with high sensitivity and selectivity, *Sensors and Actuators B: Chemical*, 2018, **259**, 380-386.

3 N. Venkatramaiah, S. Kumar and S. Patil, Fluoranthene based fluorescent chemosensors for detection of explosive nitroaromatics, *Chemical communications*, 2012, **48**, 5007-5012.
4 S. Kumar, N. Venkatramaiah and S. Patil, Fluoranthene Based Derivatives for Detection of Trace Explosive Nitroaromatics, *The Journal of Physical Chemistry C*, 2013, **117**, 7236-7245.
5 A. Sil, D. Giri and S. K. Patra, Arylene–vinylene terpyridine conjugates: highly sensitive, reusable and simple fluorescent probes for the detection of nitroaromatics, *Journal of Materials Chemistry C*, 2017, **5**, 11100-11110.
6 H. Ma, F. Li, P. Li, H. Wang, M. Zhang, G. Zhang, M. Baumgarten and K. Müllen, A Dendrimer-Based Electropolymerized Microporous Film: Multifunctional, Reversible, and Highly Sensitive Fluorescent Probe, *Advanced Functional Materials*, 2016, **26**, 2025-2031.
7 X. Gong, H. Zhang, N. Jiang, L. Wang and G. Wang, Oxadiazole-based 'on-off' fluorescence chemosensor for rapid recognition and detection of Fe2+ and Fe3+ in aqueous solution and in living cells, *Microchemical Journal*, 2019, **145**, 435-443.
8 Z. Zhang, F. Li, C. He, H. Ma, Y. Feng, Y. Zhang and M. Zhang, Novel Fe3+ fluorescence probe based on the charge-transfer (CT) molecules, *Sensors and Actuators B: Chemical*, 2018, **255**, 1878-1883.
9 X. Tang, Y. Wang, J. Han, L. Ni, L. Wang, L. Li, H. Zhang, C. Li, J. Li and H. Li, A relay identification fluorescence probe for Fe3+ and phosphate anion and its applications, *Spectrochimica Acta Part A: Molecular and Biomolecular Spectroscopy*, 2018, **191**, 172-179.
10 J. Qian, N. Huang, Q. Lu, C. Wen and J. Xia, A novel D-A-D-typed rod-like fluorescent material for efficient Fe(Ⅲ) and Cr(Ⅵ) detection: Synthesis, structure and properties, *Sensors and Actuators B: Chemical*, 2020, **320**, 128377-128381.
11 N. Kim, J. Lee, S. Park, J. Jung and D. Kim, A Schiff Base Fluorescence Enhancement Probe for Fe(III) and Its Sensing Applications in Cancer Cells, *Sensors*, 2019, **19**, 2500-2502.
12 J. Li, Q. Wang, Z. Guo, H. Ma, Y. Zhang, B. Wang, D. Bin and Q. Wei, Highly selective fluorescent chemosensor for detection of Fe3+ based on Fe3O4@ZnO, *Sci Rep*, 2016, **6**, 23558-23560.
13 H. Nawaz, W. Tian, J. Zhang, R. Jia, Z. Chen and J. Zhang, Cellulose-Based Sensor Containing Phenanthroline for the Highly Selective and Rapid Detection of Fe2+ Ions with Naked Eye and Fluorescent Dual Modes, *ACS Applied Materials & Interfaces*, 2018, **10**, 2114-2121.
14 X. Xu, D. Ren, Y. Chai, X. Cheng, J. Mei, J. Bao, F. Wei, G. Xu, Q. Hu and Y. Cen, Dual-emission carbon dots-based fluorescent probe for ratiometric sensing of Fe(III) and pyrophosphate in biological samples, *Sensors and Actuators B: Chemical*, 2019, **298**, 126829-126832.